IEEE Access
Multidisciplinary | Rapid Review | Open Access Journal

Received September 1, 2021, accepted September 15, 2021, date of publication September 20, 2021,
date of current version September 30, 2021.

Digital Object Identifier 10.1109/ACCESS.2021.3114164

A Broadband Polarized Metamaterial Absorber Driven by Strong Insensitivity and Proximity Effects

MD JASIM UDDIN[1], (Member, IEEE), MOHAMMAD HABIB ULLAH[2], AND SYED ZAHURUL ISLAM[3]

[1]Department of Applied Computing and Engineering, Cardiff School of Technologies, Cardiff Metropolitan University, Cardiff CF5 2YB, U.K.
[2]Institute of Research Management and Monitoring, University of Malaya, Kuala Lumpur 50603, Malaysia
[3]Power Integration System, Faculty of Electrical and Electronic Engineering, Universiti Tun Hussein Onn Malaysia, Parit Raja, Johor 86400, Malaysia

Corresponding author: Md Jasim Uddin (muddin@cardiffmet.ac.uk)

This work was supported in part by the School of Electrical Engineering and Computer Sciences (EECS), Queensland University of Technology, under QUTPRA and HDR Research Award.

ABSTRACT Artificial electromagnetic metamaterial produces exotic resonance, extra ordinary characteristics not available in nature, but engineers can inherit the characteristics by controlling and manipulating their structure. This research primarily the design and realization of dual-band, polarization, and incident angle insensitive metamaterial absorber (MA) is presented. By controlling and manipulating the electromagnetic design shape, artificial structure, periodic array pattern, and dielectric layer thickness a significant way to realize high absorption. In order to achieve high absorption a new shape of an octagonal ring (OR), cross-wires (CWs), and cut-off circle (CC) artificial structure have been sensibly selected. The special characteristics of this structure produce a dual resonance and its bandwidth rises compared that of classical absorber. The proposed artificial structure operation suits the Ku-band application, but possible to enhance in *C*-band. The numerical and experimental results display a dual-band 99.8% at 12.2 GHz and 99.9% at 15.5 GHz resonance is an excellent agreement in theory and numerical analysis. The effects of the constitutive property parameters: dielectric constant (ε), magnetic permeability (μ), and negative refractive index (n) are also investigated. The investigation of symmetric design structure shows the polarization-insensitivity and high absorption initiated even in changing the incident angle. Numerical and experimental results confirmed the destructive interference of multiple penetrations are responsible for the near-unity absorption. An excellent agreement in the absorptivity rates that touches near perfection which is prominent for solar cells, detection, and imaging applications.

INDEX TERMS Metamaterial absorber, constitutive parameter extraction, polarization, insensitivity, incident angle.

I. INTRODUCTION

The electromagnetic (*EM*) wave interaction with matters has become a pioneering interest and it is given considerable attention in the design prospect, fabrication, and measurement in absorber areas retrieving from microwave to optical frequency range. Recent research advances with their great attention to tune electromagnetic wave radiation without changing structural geometry. Microwave-based absorber such an example that absorb electromagnetic radiation even the changing of polarization and direction but still appear broader bandwidth. Absorbers are used in a variety of applications such as energy harvesting efficiency [1], radar imaging and reducing radar cross-section [2], thermal emission [3], sensing or enhancing detection sensitivity [4], solar cells [5], and photodetection [6]. Metamaterial-based absorbers provide unusual characteristics due to their artificial sub-lambda structure. The design specifications vary for different applications including single-, dual-, and multi-band as well as broadband frequency performance. The significant advantages of the proposed absorber structure lie in polarization insensitivity, wide incident angle, near-perfect

The associate editor coordinating the review of this manuscript and approving it for publication was Zhongyi Guo.

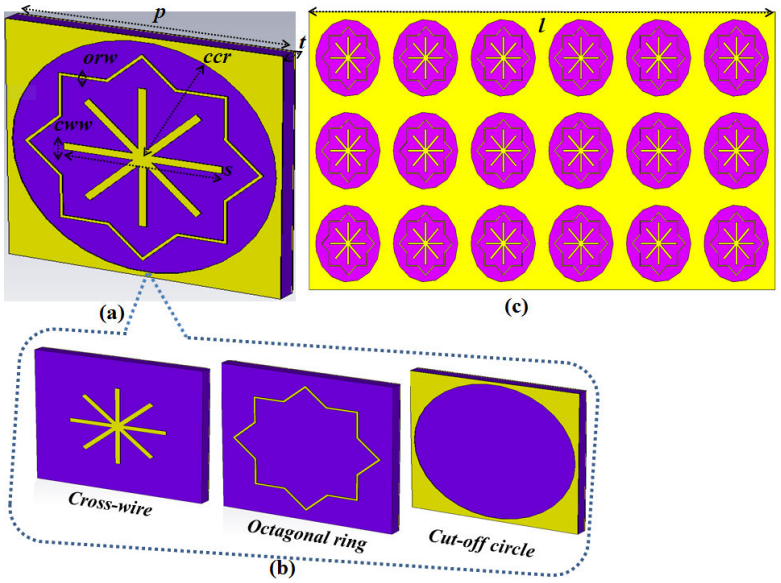

FIGURE 1. (a) The geometric representation of the metamaterial absorber for the single unit cell. (b) The three-different shape: cross-wire width (cww), octagonal ring width (orw), cut-off circle radius (ccr); (c) The periodic sample for 6 × 3 unit cell (39 mm × 78 mm), substrate FR-4, thickness, t = 1.6 mm, loss tangent $\delta = 0.02$, and dielectric permittivity $\varepsilon = 4.2$.

absorption, large bandwidth, and single to multi-band operation [7]. There are several weaknesses found in conventional absorbers. Xu and Sonkusale [8] and Li *et al.* [9], considered a metamaterial absorber using a diverse split-ring resonator feeding the patches on substrate that is more convenient in high-frequency applications. However, there are lack of investigation replicates the physical and dielectric properties on their device. Huang *et al.* [10], Alves *et al.* [11], and Landy *et al.* [12] represents a single band device with high absorption, polarization insensitivity that includes design, fabrication, and measurements. There is still a lack of investigation so far in the dual-band or multi-band metamaterial absorbers. Cheng *et al.* [13] exhibited a design that achieves a high absorption rate as well as enhanced wide-band operation. However, they etched the unit cells structure in a different way fully depended on tuning capability that results to gain and rigid to compete the high polarization and sensitivity.

In this research, we represent the design characteristics and experimental demonstration of dual resonance periodic metamaterial absorber specifically with a newly octagonal ring (OR), cross-wires (CWs), and cut-off circle (CC) shape structure which produced perfectly near unity dual resonance at 12.2 GHz and 15.5 GHz, respectively.

The design is implemented in a simple planar geometry and consists of a dual metallic layer, separated by a thin dielectric substrate. The top layer consists of an octagonal ring and crosswire located in the circular exclusion of the octagonal ring, on a dielectric substrate. The bottom layer is covered in a metallic ground plane that restricts the transmission of the absorber. Metamaterial absorber can be modified to operate at a lower frequency 6.7 GHz region (C-band).

The proposed metamaterial absorber exhibits versatile absorption characteristics due to its polarization insensitively and ability to become fully functional at different angles of incidence. Numerical and experimental results show excellent agreement and confirm the theory. The geometry of a single unit cell is shown in Figure 1 (a)-(b) along with its three different shapes: cross-wire, octagonal ring, and cut-off circle [14]. The key parameters are $s = 3$ mm, $p = 12$ mm, $t = 0.75$ mm, cross-wire width (cww) = 0.3 mm, octagonal ring width (orw) = 0.2 mm, cut-off circle radius (ccr) = 5 mm, $l = 78$ mm. A 6 × 3 periodic structure unit cell absorber is shown in Figure 1(c). In order to constraint, the cost efficiency for fabrication and etching process FR-4 substrate are selected with the thickness, loss tangent, and dielectric constant are 1.6 mm, 0.02 mm and 4.2 respectively. The periodic boundary and Floquet ports are utilized for numerical simulation and considered as infinite slabs [15], [16]. The absorption with respect to the frequency is defined as $A(\omega) = 1 - |S_{11}|^2 - |S_{21}|^2$, where $A(\omega)$ represents absorptivity, S_{11} indicates reflectivity, and S_{21} signifies transitivity. The transmission values can be reduced to near-zero absorption due to the metallic ground plane. Therefore, the reflection only considered in the calculation of the absorption. Therefore, the absorption can be calculated $A(\omega) = 1 - |S_{11}|^2$. Numerical and experimental results display that the proposed metamaterial absorber is appropriate for microwave frequency applications.

A. BOUNDARY SELECTION FOR NUMERICAL MODELLING IN WAVEGUIDE STRUCTURE

The numerical modeling and calculations are carried out using scattering parameters. The absorption $A(\omega)$ can be

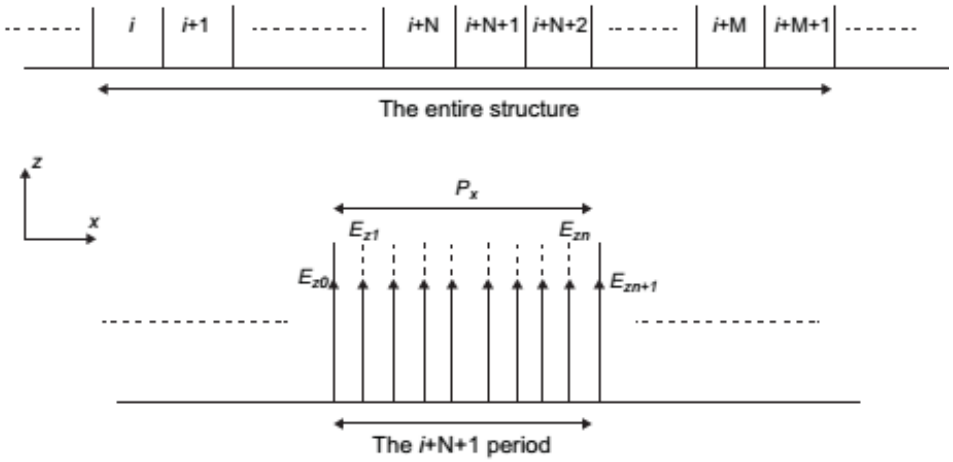

FIGURE 2. The example of periodic boundary condition structure along with periodicity in x direction.

calculated by obtaining the square of the absolute value of transmittance $T(\omega)$ and reflectance $R(\omega)$. For near-unity absorption, it is necessary to reduce transmittance $T(\omega)$ and reflectance $R(\omega)$ simultaneously. The absorber controls the incident wave by tuning electric $\varepsilon(\omega)$ and magnetic $\mu(\omega)$ resonance and should eliminate the transmitted wave. A thick metallic layer is attached to the bottom layer of the design structure, and transmittance $T(\omega)$ thus becomes zero in all the cases. The absorption can be calculated by the square of the absolute of the reflection coefficient. A periodic boundary and *Floquet ports* are selected to perform the simulation of an infinite slab in the waveguide. The Periodic boundary is selected because of boundary conditions that incorporate the large structure especially infinite structure using cascading unit-cell basis [17]–[20]. Therefore, it is essential to configure infinite structure using periodic boundary conditions as shown example in Figure 2. The waveguide ports are aligned at the front and back of the periodic unit cells absorber and it is excited on transverse electric (TE) and transverse magnetic (TM) mode. The TE wave depends on the incident angle. During the transverse electric illumination, only the tangential electric incident field attributes in direction plane $z = z_0$, where z_0 is the excitation position. This exciting single field allows the plane wave to propagate in both directions $z > z_0$ and $z < z_0$.

II. DESIGN SPECIFICATION

The proposed metamaterial absorber consists of three different layers. The top and bottom layers consist of the copper metallic sheet, the in-between layer comprises a *FR-4* substrate. The top metallic layer consists of three different shapes: the octagonal ring, cross-wire's, and cut-off circle. Each of the shapes supports a different mode of resonance. The design parameters are optimized for peak absorption. For designing microwave absorber *FR-4* substrate was selected. The bottom layer consists of a metallic sheet acting as a ground plane. Therefore, the transmission of the absorber becomes zero. Destructive interference of multiple reflections can partially explain the mechanism of absorption. Physically, the electrically thin layer produces zero backward scatterings, which can be explained in terms of multiple destructive reflections. The simulation process was performed using 2D full-wave Electromagnetic Finite element tools. The excitation of the design structure is aligned with the longitudinal plane with electric field E in the vertical plane and magnetic field H along with the horizontal plane. A periodic boundary and *Floquet* ports are used to simulate the infinite slab.

The geometric representation of a single unit cell metamaterial absorber is shown in Figure 3 (a). Numerical simulation results for an absorber with a substrate thickness of 0.75 mm is seen in Figure 3 (b). It shows two different resonances. The first resonance is found with maximum absorption up to 98% at 12.2 GHz. The second resonance displays 99% absorption at 15.5 GHz with a higher absorption peak compared to the first resonance. However, if we tune the design structure parameters, it is possible to enhance higher resonance even in lower frequency regions. Figure 3 (c) shows the single band metamaterial absorber in the highest resonance and absorption (100%) at the lower frequency of 6.7 GHz. In this substance, the same substrate are used except the thickness (t) = 1.6 mm. The dimensions of the metamaterial absorber are s = 3 mm, p = 12 mm, t = 1.6 mm, cww = 0.3mm, orw = 0.2 mm, ccr = 5 mm. The fractional bandwidth (FBW) is shown in the inset of Figure 3 (c) (inset) to observe the reflection (Γ) response of the device. The fractional bandwidth can be written as, FBW = Δf/f0, where Δf indicates the half-power bandwidth and f0 represent the center frequency. The proposed metamaterial absorber performance parameters are obtained as f0 = 6.693 GHz and Δf = 0.266 GHz, FBW = 3.9%. The fractional bandwidth results give acceptable results that are suitable for many applications [21], [22].

A fabricated sample of the metamaterial absorber with the periodic unit cell in both vertical and horizontal is shown in Figure 4 (a). The numerical and experimental results of a

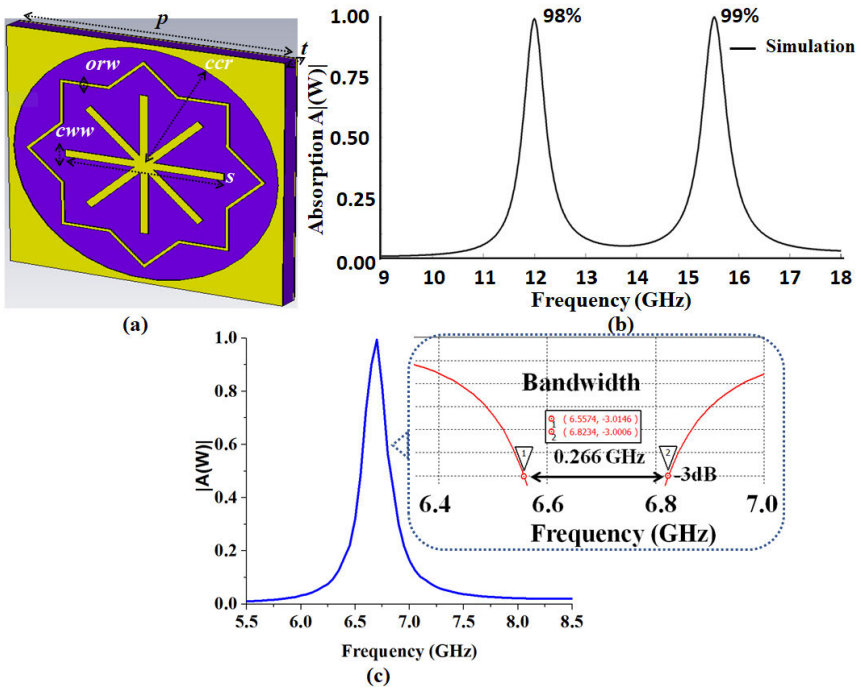

FIGURE 3. (a) The single unit cell metamaterial absorber; (b) Numerical results of single unit-cell metamaterial absorber with dual band operation when thickness t = 0.75mm; (c) Simulation results of metamaterial absorber in single band operation while increasing thickness t = 1.6mm. [parameters: cross-wire width (cww), octagonal ring width (orw), cut-off circle radius (ccr)].

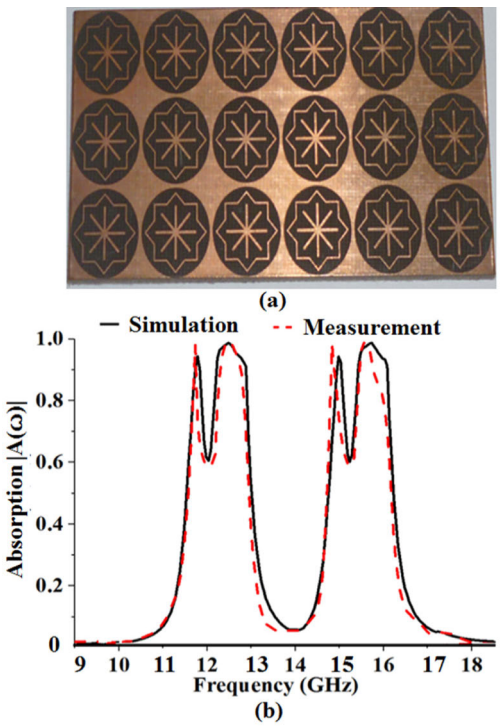

FIGURE 4. (a) The photograph of prototype fabricated sample for 6 × 3 periodic unit cell (width × length, 39mm × 78mm); (b) Simulation and measurement results of metamaterial absorber with dual wide-band operation during 6 × 3 periodic unit-cell.

6 × 3 periodic unit-cell structure are shown in Figure 4(b). The geometric parameters dimension representation of the metamaterial absorber is length (l) = 62.4 mm, p = 12 mm, t = 1.0 mm, orw = 0.2 mm, cww = 0.3 mm, s = 3.0 mm, ccr = 5 mm. It shows wide bandwidth when the number of unit cells is increased. Here, p is the single unit cell spacing of the structure and acting as a periodic repetition replaced by an effective medium where each unit cell size is much smaller than the wavelength. The periodic array produces electric and magnetic resonance.

The absorption is shown in Figure 4 (b) has a dual resonance at 12.2 GHz and 15.5 GHz. It does not shift the center resonance frequency even in a periodic structure, because increasing the number of unit cells does not affect the electromagnetic element (electric and magnetic resonance).

This periodic structure has generally enhanced the bandwidth. Figure 4 (b) exhibits a small discontinuous resonance due to the close center to center unit-cell distance. The continuous wider band is possible by adjusting the distance between the unit cells. The objective of the proposed design is to compare the single and periodic unit-cell structure and showing that an increase in the number of unit cells varies the bandwidth of the structure.

A. EFFECTS OF TE, TM MODES, AND CONSTITUTIVE PARAMETER EXTRACTION

The metamaterial-based absorber has attracted special attention due to its strong resonance, multiband and broadband characteristics while not requiring any thick material of the structure. When the electromagnetic incident wave *TE* and *TM* mode is polarized, it becomes a challenge to make it

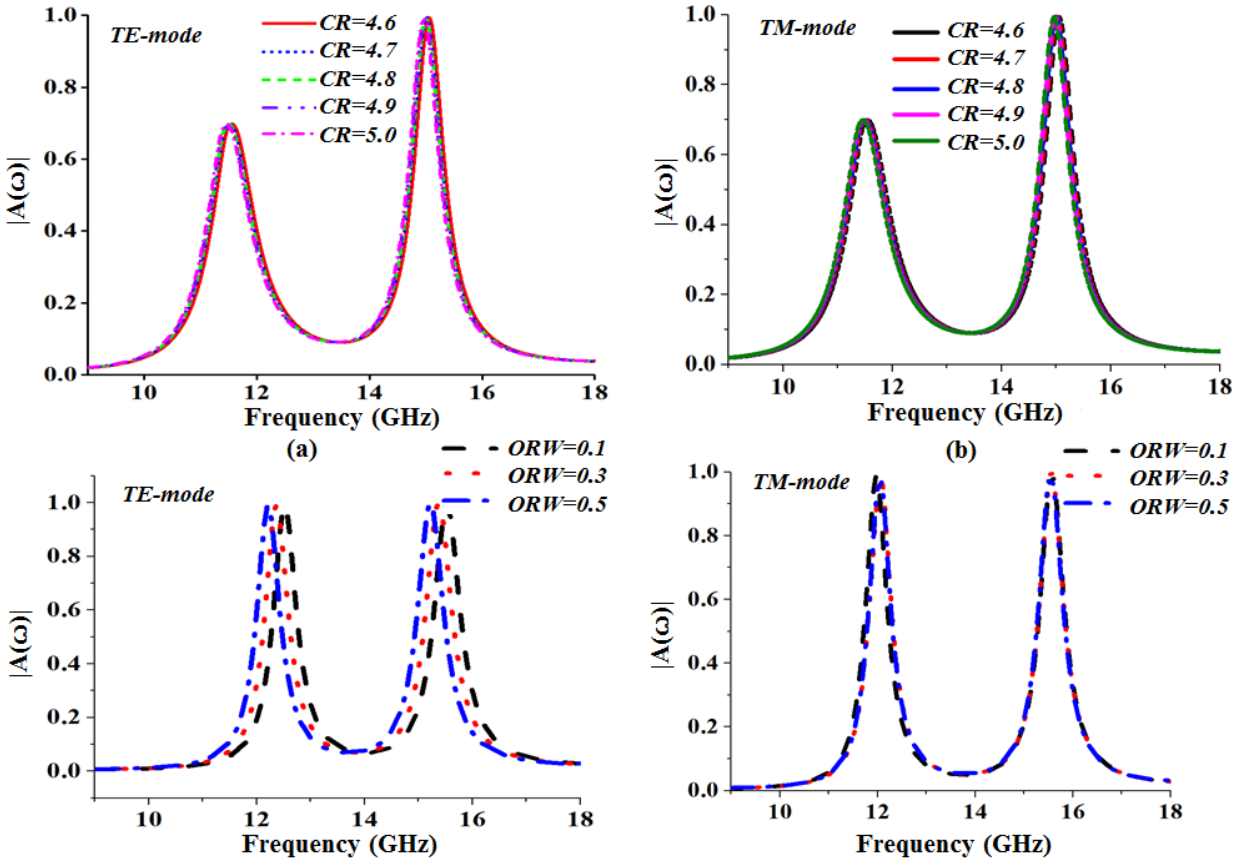

FIGURE 5. The absorption values of copper patch radius parameters from 4.6mm to 5.0mm for (a) TE and (b) TM modes of incidence angle. Effects of the proposed structure metamaterial absorber changed OR width from 0.1mm to 0.5 mm with other parameters keep unchanged for (c) TE and; (d) TM mode incident radiation. [parameters: cross-wire ring (CR), octagonal ring width (ORW)].

insensitive. The objective of this research is to observe the response to transverse electric (*TE*) and transverse magnetic (*TM*) waves when rotating the structure. This should not affect the structure's absorptivity. Initially, the effects of cross-wire rings (*CRs*) are investigated for both *TE* and *TM* modes operation. Figure 5 (a) shows the first resonances that are reduced to a 70% absorption peak rate while a high absorption peak of 99% to 100% is observed at the higher peak. In the *TE* mode analysis, the results of cross-wire ring parameters are chosen from 4.6 mm to 5.0 mm, where individual parameter graph shows very minimum distance to each other. It shows the second resonance drifts to a higher frequency from 15 GHz to 15.4 GHz. Figure 5 (b) shows that resonance for the *TM* mode for cross-wire rings is almost as same as for the *TE* mode. The only difference compared to *TE* modes is that the second resonance maximum peak shifted varying from 99%∼100% at higher frequencies. Further investigation on the effects of the octagonal ring width (*ORW*) for normal incidence angle in both *TE* and *TM* polarization is obtained. Figure 5 (c) shows that the absorption changes for ring width varying from 0.1 mm to 0.5 mm for *TE* modes. In *TE* mode analysis, both the first and second resonance absorption frequency and peaks are sensitive to the octagonal ring width. It shows drifting in higher frequency when the octagonal ring width changes. At *TM* mode analysis is shown in Figure 5 (d), where the absorption is largely insensitive to the octagonal ring width. Here, the second resonance absorption peak is higher than the first resonance peak. Furthermore, the discussion includes the effect of cross-wire width (*CWW*) of the absorber varying from 0.2 mm up to 0.4 mm while the other parameters remain unchanged. The parametric analysis is done both in *TE* and *TM* mode operation, as shown in Figure 6. In *TE* mode polarization, it shows when the cross-wire width becomes large, the resonances are almost similar in width with an absorption peak of 99.2%, details of which are shown in Figure 6 (a). On the other hand, for *TM* mode polarization, the resonance frequencies drift to higher frequencies. The resonance is shifted to higher frequencies when the cross-wire reduces in its width. However, the peak absorption remains near to 100%, as shown in Figure 6 (b). The further investigation involves discussion on the effect of incidence angle in both *TE* and *TM* modes polarization with results shown in Figure 6 (c)-(d). Due to the symmetrical design structure, the metamaterial absorber is largely insensitive to polarization. It is critical to observe the situation from a different angle of incidence performance. The theoretical behaviour should be stable even when the incidence angle

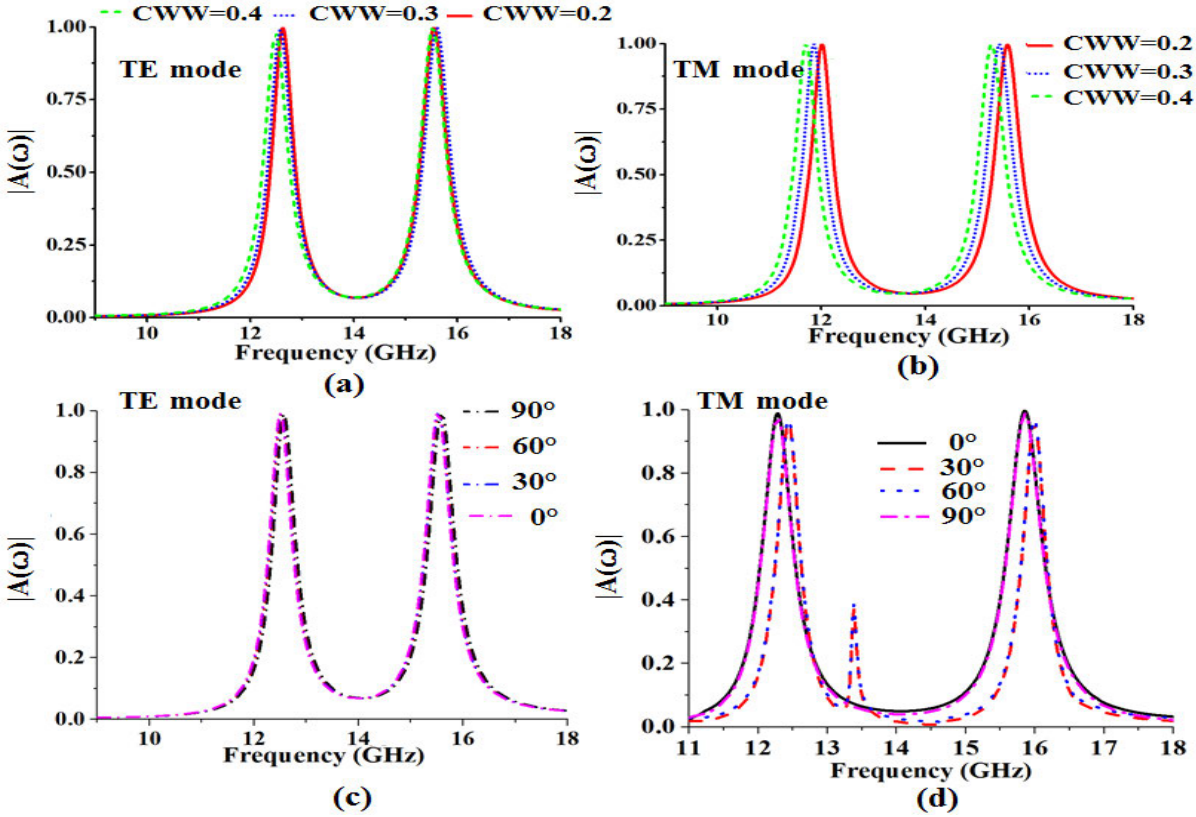

FIGURE 6. (a) Effects of the proposed structure MA changed the cross-wire width (CWW) from 0.2mm to 0.4 mm with other parameters keep unchanged for (a) TE mode incident radiation; (b) TM mode incident radiation. The absorber performance analysis for different polarization angle is investigated in the case of normal incidence: (c) TE polarization angle; (d) TM polarization angle.

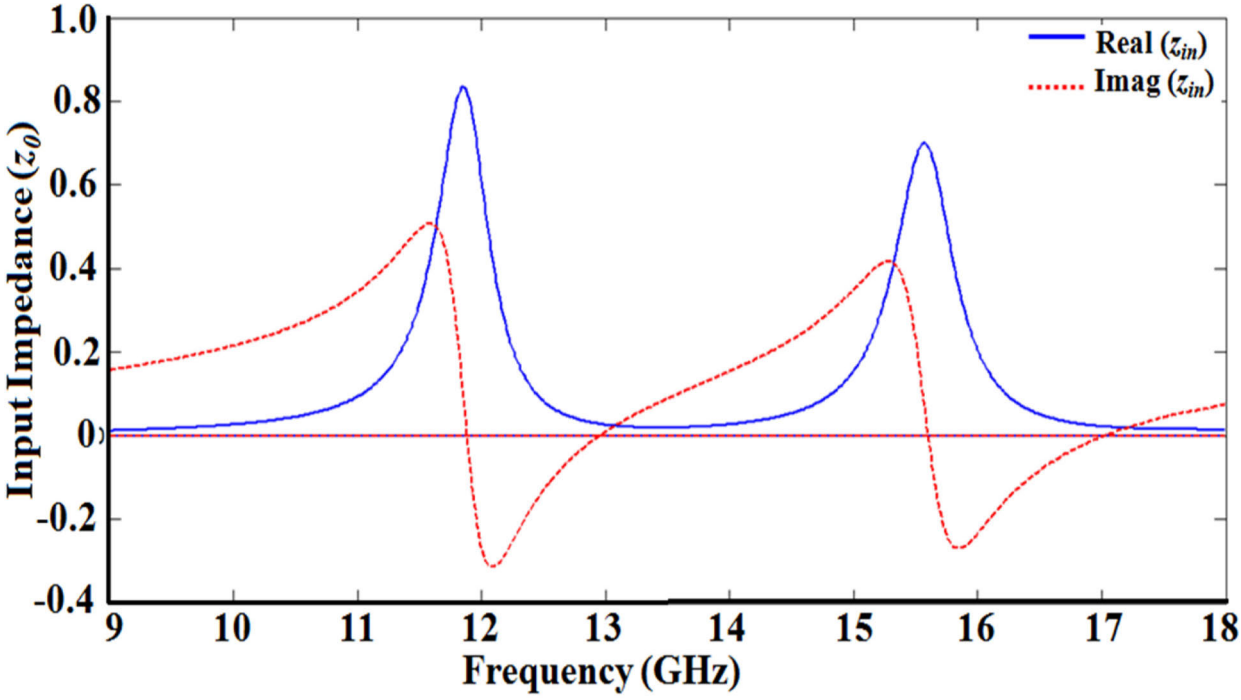

FIGURE 7. The real and imaginary part of the impedance.

is changed. Figure 6 (c) illustrates that the absorption in *TE* mode is about 98.5% at the lower order resonance frequency and 99.7% at the higher frequency. The different incidence angles did not affect resonance, which ensures versatility.

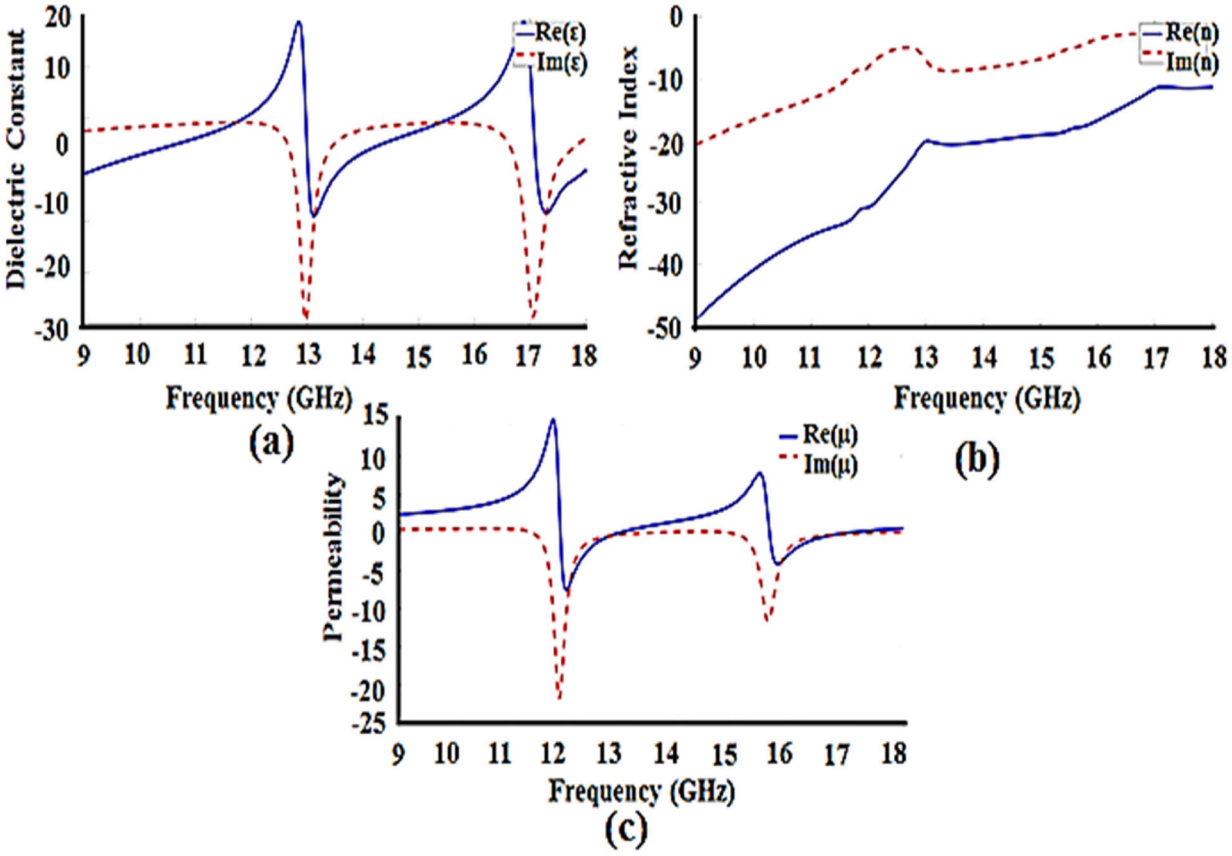

FIGURE 8. (a) Numerical analysis of constitutive electromagnetic properties: dielectric permittivity (b) negative refractive index and (c) magnetic permeability response.

However, in *TM* mode analysis, first and second resonance frequency have experience some shifting while the incidence angles are changed. While the dual resonance absorption shifted, its peak values are also decreased. A new series of tiny ripples can be seen around 13.4 GHz up to 13.6 GHz as shown in Figure 6 (d). In *TM* mode analysis, an acceptable absorption rate (98.6%) is found in 0° and 90° respectively, where at other incident angles 30° and 60°, absorption peaks drop to 96.5%. We also investigated the electromagnetic properties of metamaterial absorbers to extract the dielectric constant, magnetic permeability, and refractive index. Since the wave propagates along the longitudinal axis, the distance d implies a phase change of $(2\pi d/\lambda)$, where λ is the wavelength of the structure [23], [24]. The boundary conditions and excitations are assigned to different surfaces of the microstrip unit-cell element to simulate the periodic metamaterials. For a plane, electromagnetic incident wave with the scattering parameters of the reflection coefficient R can be written as $S_{11} = Re^{ik0d}$. The k_0 denotes the incidence wave number in free space.

By adjusting the physical parameters of the top metallic conducting layer, and the modification of the dielectric substrate, both electric and magnetic responses can be tuned in a specific frequency region. Thus, the input impedance (z_{in}) of the structure becomes matched with the free space of the impedance (z_0) using the following expression [25]–[27]:

$$z_{in} = z_0 \frac{(1 + s_{11})}{(1 - s_{11})} \tag{1}$$

In Figure 7 shows that the imaginary part of the input impedance is nearly zero at the two resonance frequencies. Thus, the incident wave can get into the absorber without reflection under the matching condition. The absorber mainly absorbs in the resonance frequency region because the electric field is tuned to match the free space impedance, thus achieving near-perfect absorption.

The material parameters of the proposed design are extracted using the modified Nicholson-Ross-Weir *(NRW)* technique [25]. There are two resonant frequency ranges (f_1 = 11-13.2 GHz) and (f_2 = 14.5-17 GHz), which were investigated to extract the constitutive electromagnetic parameters. They exhibit unusual electromagnetic parameters. There is a resonant behaviour of the real part of the dielectric permittivity, being negative at both f_1 and f_2. The imaginary part is near-zero value, except at the dual resonance frequencies (f_1, and f_2), where the values are negative. Figure 8 (a) shows the real and imaginary parts only at the first and second resonance. It shows the real part of dielectric permittivity becomes negative at the resonance frequencies. The imaginary parts are close to zero except at

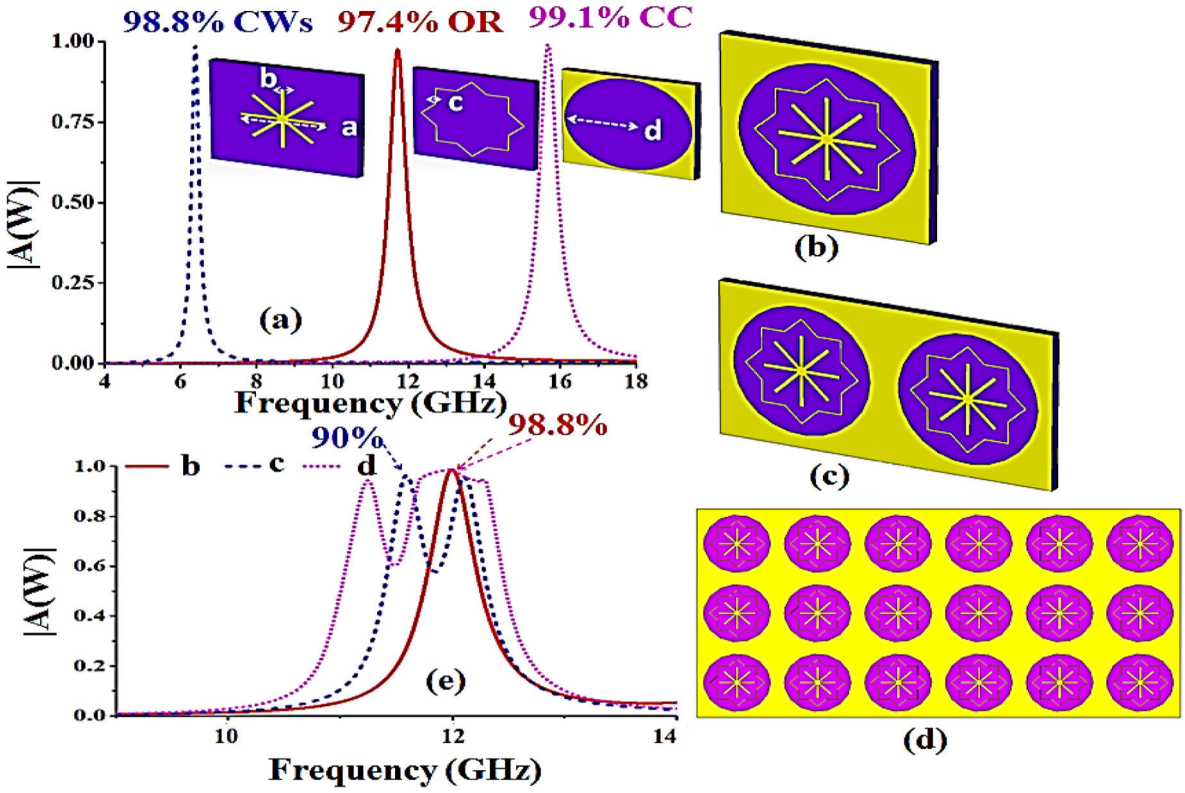

FIGURE 9. (a) The contribution of different structure performance analysis of proposed structure [Cross-wire (CW), Octagonal Ring (OR), Cut-off Circle (CC)]. (b) the single unit cell dimension parameters are p = 10.4 mm, t = 0.75 mm, ORW = 0.2 mm, CWW = 0.3 mm, S = 3.0 mm, CR = 5.0 mm; (c) double unit cells parameters are p = 20.8 mm, t = 1.0 mm, ORW = 0.2mm, CWW = 0.3mm, S = 3.0 mm, CR = 5.4 mm. (d) The design of 6 × 3 unit cells parameter geometry are: p = 62.4 mm, t = 1.0 mm, ORW = 0.2 mm, CWW = 0.3 mm, S = 3.0 mm, CR = 5.6mm. (e) The comparison absorption performance of single, two, and 6 × 3 periodic unit-cells, respectively.

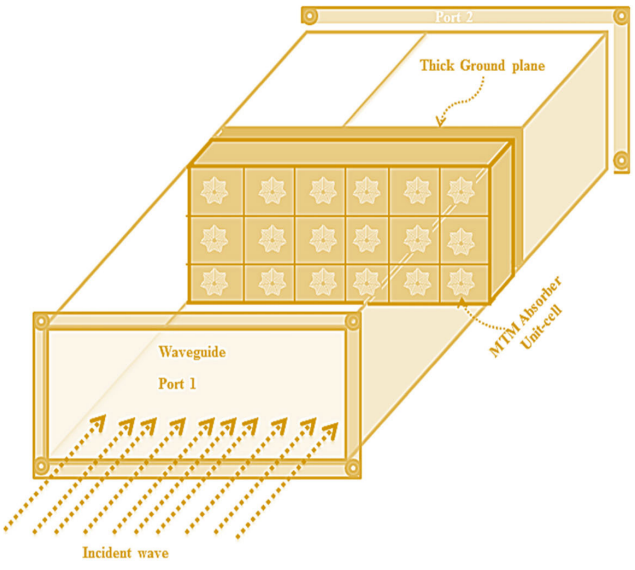

FIGURE 10. The test absorber sample is placed and mounted on the standard waveguide structure.

the resonance frequencies where it becomes negative. The imaginary part also represents the loss factor and energy absorbed. The refractive index becomes negative over the entire frequency region. Figure 8 (b) shows the negative refractive index in both resonance frequency regions. The negative refractive index confirms that the proposed design shows the left-handed (*LH*) behaviour of metamaterials. The real and imaginary part of the relative permeability is shown in Figure 8 (c). The real part shows negative magnetic resonance at the two resonance frequencies. The imaginary parts show near to zero values except at the resonance frequencies. The magnetic permeability can be retrieved by using the combination of refractive index and wave impedance.

B. STRUCTURE ANALYSIS AND BANDWIDTH ENHANCEMENT

The individual structure behaves with maximum absorption of different frequencies. The first absorption peak is achieved from the cross-wires. The design specification and parameter values are given in detail in Figure 9 (a). The absorption peak is found at about 98.8% at 6.25 GHz. The octagonal ring that is feeding on top of the substrate is another structure of the design. The obtained design structure produced a higher resonance mode compared to the cross-wire. In order to achieve high resonance, the metallic ring width is adjusted

($c = 0.2$ mm). The absorption peak shifted resonance 97.4% at 12 GHz.

The cut-off circle etched on the substrate gives the third resonance near 16 GHz, as shown in Figure 9 (a). The design structure shows an absorption rate of 99.1 %, which is higher compared to the other structures. The maximum absorption peak is found when the adjusted radius (d) is 5mm. It was found that increasing the number of unit-cell increased the bandwidth significantly. The three individual components provide the perfect dual resonance with a high peak. The single unit-cell represents a high absorption peak rate of 98.8% at 12.2 GHz resonance frequency, as shown in Figure 9 (b).

The fractional bandwidth of the single unit cell of 0.05% at −3 dB. By improving the bandwidth performance, two-unit cells are considered, as shown in Figure 9 (c). The entire cell size increases up to 20.8 mm and a width of 2.0 mm is selected. The design structure shows a higher bandwidth than the previous structure. An absorption peak of 90% was found and the fractional bandwidth improved to 0.08% at −3dB. Furthermore, 6 × 3 periodic unit cells are realized in Figure 9(d). In the periodic structure, the unit-cell size is 62.4 mm and a substrate thickness of 1.0 mm was used. A modified cut-off circle patch of 5.6 mm is found through optimization. The periodic unit cells that shown a high absorption peak are identical to the single unit-cell with the absorption of 98.8% at 11.75 GHz. The fractional bandwidth was found to be 0.14% at -3 dB. A comparison result of the single unit cell, dual unit-cell, and periodic 6 × 3 unit-cell are shown in Figure 9 (e).

III. EXPERIMENT SETUP

The proposed metamaterial absorber consists of three distinct resonators: cross wire, octagonal, and cut-off circle rings. The design is constructed metallic layers on top and bottom sides, which are separated by a lossy *FR-4* substrate. The periodic 6 × 3 unit-cell design is fabricated through standard printed circuit board (*PCB*) technology. In the experimental setup, the absorber performance was verified in the closed system waveguide method as shown in Figure 10. The absorber sample is placed into the waveguide (*WR137*) perpendicularly, and two ports are connected to an Agilent vector network analyzer to receive the waves that represent the magnitude of the sample sheet. A thick metallic ground plane is inserted to prevent the transmitted wave, *i.e.*,, $S_{21} = 0$. Therefore, only the reflection data is collected to obtain the absorptivity. To prevent leakage, both ports are covered with a thick metal plane. During the excitation, all reflection is diminished and thus the incident wave is absorbed. Figure 11 shows the simulation and measurement results of the reflection coefficient for the proposed periodic 6 × 3 metamaterial absorber structure.

When the electromagnetic incident wave passes through the structure, the absorbance can be calculated as $A(\omega) = 1 - |S_{11}(\omega)|^2 - |S_{21}(\omega)|^2$, where $A(\omega)$, $|S_{11}(\omega)|^2$, and $|S_{21}(\omega)|^2$ are the absorbed, reflected, and transmitted power. The proposed absorber bottom layer is attached to a thick metallic layer. Therefore, there is zero transmission through the structure and the full power can be absorbed. The absorptivity expression is then can be written as $A(\omega) = 1 - |S_{11}(\omega)|^2$. Therefore, we can significantly improve the electric and magnetic resonance in specific frequency regions by adjusting physical constraints through tuning the physical parameters of the top layer as well as the thickness of the dielectric substrate layer. The input impedance $Z(\omega)$ of the structure is then perfectly matched to the free space of impedance Z_0. According to Reference [28] and [29] the excitation of incident energy is absorbed as on-center and off-center, respectively. In this case, the on-center incident energy attracted to the structure without reflections.

A. THE INCIDENT ENERGY AND POWER DISSIPATION

The conventional microwave absorber consists of a thick metallic backplate, for example, a single resistive sheet [30], or a double resistive sheet [31] to eliminates the transmission power through the absorber. Metamaterial absorber is easy to integrate and flexible to make ultra-thin structure along with near-unity absorption. The lossy high impedance surface is capable of high absorption. By changing the top layer of the parametric structure, resonance can be modified to a different frequency either dual-band or multi-band. By tuning electric and magnetic resonance, the metamaterial can match the input impedance to the free space impedance. The multi-layer structure also eliminates the transmission of power ($T = 0$). Thus, the highest peak of 100% absorbance is possible. In order to replace the metallic resistive sheets, several resonating inclusions and geometric parameters on the top layer are one of the solutions to eliminate the power transmission [32]. The additional metallic ground layer also can be used to minimize the transmission. In that case, a metamaterial absorber needs to be designed in such a structure where the imaginary part of permeability (μ) and dielectric constant (ε) as large as possible. This is because they are correspondence to the loss in the artificial structure. The maximum power can be absorbed by reducing the reflection and transmission of the absorber structure. In general, a strong absorption power is achieved in the resonance region where the structure is properly excited.

The power dissipated in the proposed electromagnetic metamaterial absorber can be achieved under three conditions: dielectric energy loss, magnetic energy loss from the substrate, and ohmic energy loss from the metal [32]–[34]. The absorption is from the dielectric energy losses occurred while the nonmagnetic materials like *FR-4* are used as the substrate. According to the literature study [35]–[37], the substrate *FR-4* where the loss tangent 0.02 was selected to characterize the design structure. During the experiment, the major dielectric loss can be found in order to use lossy substrate. Thus, the loss can be reduced by using low lossy substrate. The *FR-4* substrate with the loss tangent ($\tan\delta$)

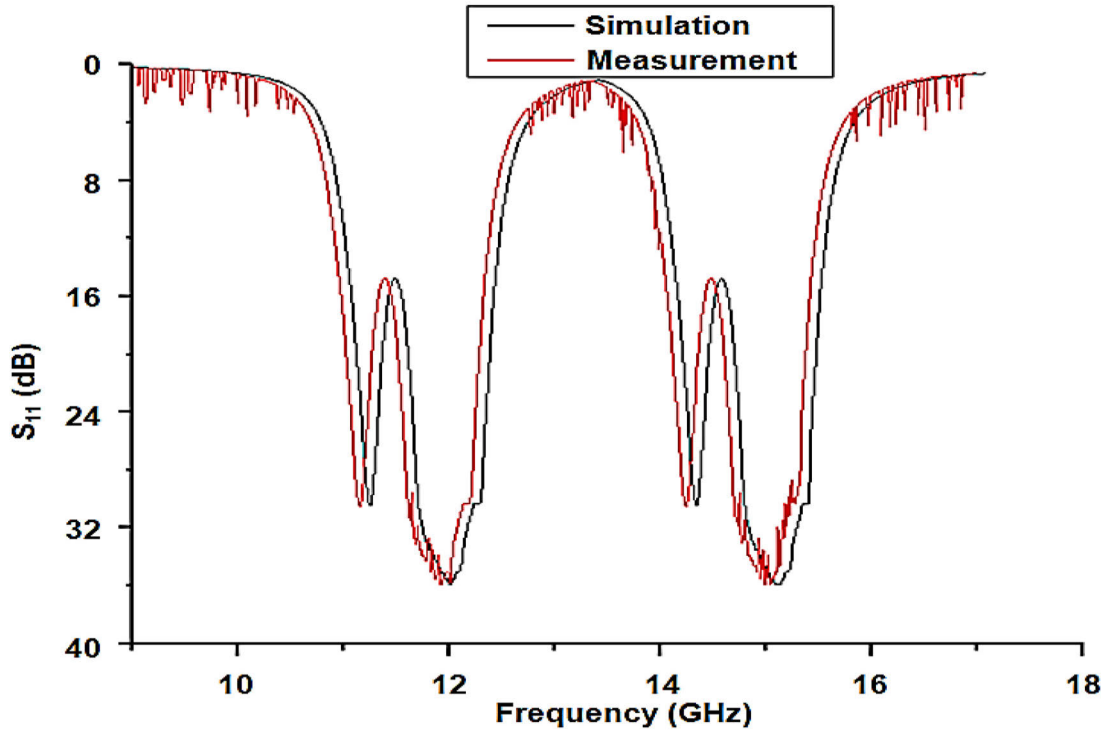

FIGURE 11. Simulation and measurement of the reflection coefficient for the proposed periodic metamaterial absorber structure.

0.02, thickness (t) 1.6 mm, and dielectric constant (ε) 4.2 are selected to this experiment. The incident power of the device is absorbed by the electric field $|E_z|$ and magnetic field $|H_z|$ [38]. The nonmagnetic material (*dielectric*) substrate is very important for metamaterial absorbers to achieve near-unity absorption. This implies a strong absorption in the high resonance region. The absorbing power is thus calculated from the substrate, the imaginary part of the dielectric constant. When the structure is fully absorbed, there are numerous electrons stored in the conduction band and holes in the balanced band that results in ionization are Fermi-distributions at room temperature [22], [39]. The calculation of the rate performance of the entire absorber device is considering in the following expression, where all in incidence radiation is absorbed without reflection, outside distributed radiations bend and recenter into the structure.

$$\eta = P_{absorb}/P_{in}, \quad P_{absorb} = -\frac{1}{2}Re\left(\oint \vec{E} \times \vec{H} \cdot d\vec{S}\right) \quad (2)$$

Here, P_{absorb} is the net power entering the absorber structure, P_{in} is the incident power, η is the efficiency of the absorber structure. The incidence power can be calculated using the contour integral of distributed receiving electric and magnetic fields. The dielectric energy loss can be calculated $P_e = (1/2)\ \omega\varepsilon''|E|^2$. Here, E is the electric field in the substrate and ε'' represents the imaginary part of permittivity.

The P_e is strongly dominated by the electric field E of the material that can be determined by the metamaterial structure, and therefore, the individual unit cell is very important in the metamaterial structure design. When a magnetic material P_m is used into substrate the absorption becomes both dielectric and magnetic energy losses. In these case, the total electromagnetic energy dissipation can be written as $P_{total} = P_e + P_m = (1/2)\,\omega\varepsilon''|E|^2 + (1/2)\omega\mu''|H|^2$. Here, H is the magnetic field in the substrate, and μ'' represents the imaginary part of permeability. We have tuned both the permeability and permittivity parameters which are equivalent to each other to become near unity absorbers. Therefore, the losses can be measured and obtained from the imaginary part of the dielectric permittivity. It is noted that the investigation involving power incidence radiation is carried out only for the theoretical interest. As the proposed metamaterial absorber unit cells are smaller than the wavelength, it is generally convenient to produce effective permeability, permittivity, and refractive index extracted from the material. The imaginary part of the permeability $\mu(\omega)$, permittivity $\varepsilon(\omega)$, and refractive index $n(\omega)$ as large as possible to obtain near-unity absorption. High electromagnetic loss can be accomplished through a large resonant imaginary part of the refractive index. In such a way, at most electromagnetic energy absorption is possible to accomplish by minimizing the transmittivity, and reflectivity [40]–[42]. The maximize absorption electromagnetic incident energy is then converted into heat. If the structure becomes thick, the resonance can trap the electromagnetic energy, where all electromagnetic

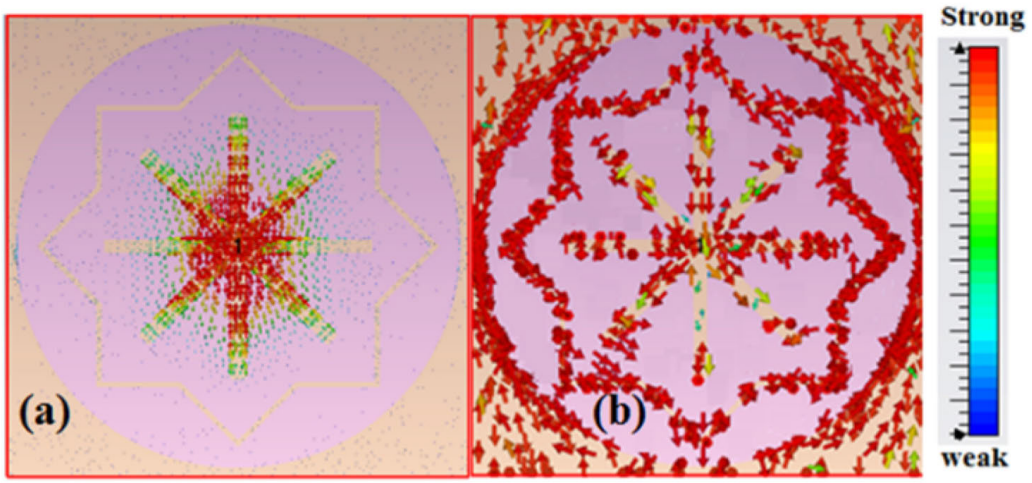

FIGURE 12. (a)-(b) surface current distribution within dual mode resonance frequencies metamaterial absorber structure ($f_1 = 12$ GHz, and $f_2 = 15.52$ GHz).

wave is absorbed and converted into the dissipated heat. The generating heat can be then controlled and detected in many ways [43]–[46] such as external diodes in electromagnetic energy harvesting, photoconductive antennas.

B. SURFACE CURRENT DISTRIBUTION

To explain the mechanism of absorption, the surface current distributions are investigated. The dual modes of current distributions at $f_1 = 12.2$ GHz and $f_2 = 15.5$ GHz are shown in Figure 12 (a) - (b).

At the lower resonance in Figure 12 (a), the circulating currents on the regions of the cross-wire structure as clearly visible. It shows prominent current distributions at the center cross point rather than the outbound wire region. High absorption and bandwidth enhancement appear at the lower resonance frequency. Due to the symmetrical design, higher resonant frequencies are achieved. Surface currents appear in metallic conductors and circulating loops around the conducting strip. It provides a magnetic field and strong magnetic coupling whereas the equivalent electric coupling appears on the metallic conducting patch areas. Details are shown in Figure 12 (b). At this frequency, both electric and magnetic resonance are excited equally and therefore high absorption is realized. The experiment is investigated large oblique incident angles up to $90°$ for both *TE* and *TM* mode excitation. It shows the graph does not shift much even the changing incident angles. Therefore, the proposed metamaterial absorber is claimed as polarization insensitive.

IV. CONCLUSION

In summary, we presented a near unity, perfect metamaterial absorber that demonstrated numerically, experimentally, and theatrically. The results show a near-unity perfect absorber with dual resonance due to their special shape: octagonal ring (OR), cross-wires (CWs), and cut-off circle (CC). These special geometry, shape and structure produce the highest resonance and due to the metallic ground substance transmission wave diminishes to zero while the absorber receives all reflective waves with their minimum interference. The proposed absorber also considered the polarization and various incident angles and the result shows still insensitive with minimum effects and brilliant adaptivity. The experiments results show an excellent absorption peak rate in the dual-mode operation of 99.8% at 12.2 GHz and 99.9% at 15.5 GHz. To extend the parameter for miniaturization, a spurious single band is possible to absorb 100% peak at 6.6 GHz. The constitutive parameters of the design structure have been analyzed to observe the effect of metamaterial behaviour. A periodic unit-cells on the other hand enhance the resonance width which builds the proposed absorber to become a competitive and prominent candidate. Least to say, these extraordinary features of artificial metamaterial absorber are promising candidates for solar cells, detection, and imaging applications.

REFERENCES

[1] M. Oudich and Y. Li, "Tunable sub-wavelength acoustic energy harvesting with a metamaterial plate," *J. Phys. D, Appl. Phys.*, vol. 50, no. 31, Aug. 2017, Art. no. 315104.
[2] J. Wang, D. Feng, Z. Xu, Q. Wu, and W. Hu, "Time-domain digital-coding active frequency selective surface absorber/reflector and its imaging characteristics," *IEEE Trans. Antennas Propag.*, vol. 69, no. 6, pp. 3322–3331, Jun. 2021.
[3] C. Xu, S. Qu, Y. Pang, J. Wang, M. Yan, J. Zhang, Z. Wang, and W. Wang, "Metamaterial absorber for frequency selective thermal radiation," *Infr. Phys. Technol.*, vol. 88, pp. 133–138, Jan. 2018.
[4] S. Tan, F. Yan, W. Wang, H. Zhou, and Y. Hou, "Ultrasensitive sensing with three-dimensional terahertz metamaterial absorber," *J. Opt.*, vol. 20, no. 5, May 2018, Art. no. 055101.
[5] M. Malitckaya, H.-P. Komsa, V. Havu, and M. J. Puska, "Effect of alkali metal atom doping on the $CuInSe_2$-based solar cell absorber," *J. Phys. Chem. C*, vol. 121, no. 29, pp. 15516–15528, Jul. 2017.
[6] L. Zhou, C. Zhang, L. Li, T. Liu, K. Li, S. Wu, and X. Li, "Nanobowls-assisted broadband absorber for unbiased Si-based infrared photodetection," *Opt. Exp.*, vol. 29, no. 10, pp. 15505–15516, 2021.

[7] Z. Guo, X. Yang, F. Shen, Q. Zhou, J. Gao, and K. Guo, "Active-tuning and polarization-independent absorber and sensor in the infrared region based on the phase change material of $Ge_2Sb_2Te_5$ (GST)," *Sci. Rep.*, vol. 8, no. 1, p. 12433, Aug. 2018, doi: 10.1038/s41598-018-30550-2.

[8] W. Xu and S. Sonkusale, "Microwave diode switchable metamaterial reflector/absorber," *Appl. Phys. Lett.*, vol. 103, no. 3, Jul. 2013, Art. no. 031902, doi: 10.1063/1.4813750.

[9] W. Li, T. Wu, W. Wang, J. Guan, and P. Zhai, "Integrating non-planar metamaterials with magnetic absorbing materials to yield ultra-broadband microwave hybrid absorbers," *Appl. Phys. Lett.*, vol. 104, no. 2, Jan. 2014, Art. no. 022903, doi: 10.1063/1.4862262.

[10] L. Huang, D. R. Chowdhury, S. Ramani, M. T. Reiten, S.-N. Luo, A. K. Azad, A. J. Taylor, and H.-T. Chen, "Impact of resonator geometry and its coupling with ground plane on ultrathin metamaterial perfect absorbers," *Appl. Phys. Lett.*, vol. 101, no. 10, 2012, Art. no. 101102, doi: 10.1063/1.4749823.

[11] F. Alves, B. Kearney, D. Grbovic, N. V. Lavrik, and G. Karunasiri, "Strong terahertz absorption using SiO_2/Al based metamaterial structures," *Appl. Phys. Lett.*, vol. 100, no. 11, Mar. 2012, Art. no. 111104, doi: 10.1063/1.3693407.

[12] N. I. Landy, S. Sajuyigbe, J. J. Mock, D. R. Smith, and W. J. Padilla, "Perfect metamaterial absorber," *Phys. Rev. Lett.*, vol. 100, May 2008, Art. no. 207402, doi: 10.1103/PhysRevLett.100.207402.

[13] Y. Z. Cheng, W. Withayachumnankul, A. Upadhyay, D. Headland, Y. Nie, R. Z. Gong, M. Bhaskaran, S. Sriram, and D. Abbott, "Ultrabroadband plasmonic absorber for terahertz waves," *Adv. Opt. Mater.*, vol. 3, no. 3, pp. 376–380, 2014.

[14] M. Uddin, "Synthesis and analysis of metamaterial structure for microwave frequency applications," Ph.D. dissertation, Queensland Univ. Technol., Brisbane, QLD, Australia, 2017.

[15] M. J. Uddin, M. H. Ullah, T. A. Latef, and W. N. L. Mahadi, "Inversion response to optimize lumped-element circuits for metamaterial," *Int. J. Circuit Theory Appl.*, vol. 45, no. 1, pp. 36–46, Jan. 2017.

[16] M. J. Uddin, M. H. Ullah, T. A. Latef, W. N. L. Mahadi, and M. T. Islam, "Making meta better: The synthesis of new-shaped periodic artificial structures suitable for metamaterial behavior characterization," *IEEE Microw. Mag.*, vol. 17, no. 8, pp. 52–58, Aug. 2016.

[17] M. H. Ullah, M. R. Ahsan, W. N. L. W. Mahadi, T. A. Latef, and M. J. Uddin, "Isolation improvement of dual feed patch antenna by assimilating metasurface ground," *Microw. Opt. Technol. Lett.*, vol. 57, no. 6, pp. 1406–1409, Jun. 2015.

[18] M. H. Ullah, W. N. L. Mahadi, T. A. Latef, M. T. Islam, M. J. Uddin, and M. R. Ahsan, "Mutual coupling reduction of dual port antenna using zero index metasurface structure," *Int. J. Appl. Electromagn. Mech.*, vol. 49, no. 3, pp. 387–394, Nov. 2015.

[19] J. Burch, J. Ma, R. I. Hunter, S. A. Schulz, D. A. Robertson, G. M. Smith, J. Wang, and A. Di Falco, "Flexible patches for mm-wave holography," *Appl. Phys. Lett.*, vol. 115, no. 2, Jul. 2019, Art. no. 021104, doi: 10.1063/1.5109627.

[20] K. Cheng, Z. Hu, Y. Wang, J. Ma, and J. Wang, "High-performance terahertz vortex beam generator based on square-split-ring metasurfaces," *Opt. Lett.*, vol. 45, no. 21, pp. 6054–6057, 2020.

[21] H. Lv, Z. Yang, H. Xu, L. Wang, and R. Wu, "An electrical switch-driven flexible electromagnetic absorber," *Adv. Funct. Mater.*, vol. 30, no. 4, 2020, Art. no. 1907251.

[22] C. Ma, C. Wang, B. Gao, J. Adams, G. Wu, and H. Zhang, "Recent progress in ultrafast lasers based on 2D materials as a saturable absorber," *Appl. Phys. Rev.*, vol. 6, no. 4, Dec. 2019, Art. no. 041304.

[23] Z. Yi, J. Chen, C. Cen, X. Chen, Z. Zhou, Y. Tang, X. Ye, S. Xiao, W. Luo, and P. Wu, "Tunable graphene-based plasmonic perfect metamaterial absorber in the THz region," *Micromachines*, vol. 10, no. 3, p. 194, Mar. 2019.

[24] M. L. Huang, Y. Z. Cheng, Z. Z. Cheng, H. R. Chen, X. S. Mao, and R. Z. Gong, "Design of a broadband tunable terahertz metamaterial absorber based on complementary structural graphene," *Materials.*, vol. 11, no. 4, p. 540, 2018.

[25] O. Luukkonen, S. I. Maslovski, and S. A. Tretyakov, "A stepwise Nicolson-Ross-weir-based material parameter extraction method," *IEEE Antennas Wireless Propag. Lett.*, vol. 10, pp. 1295–1298, 2011, doi: 10.1109/LAWP.2011.2175897.

[26] U. C. Hasar and M. Bute, "Method for retrieval of electromagnetic properties of inhomogeneous reciprocal chiral metamaterials," *IEEE Trans. Antennas Propag.*, vol. 68, no. 7, pp. 5714–5717, Jul. 2020, doi: 10.1109/TAP.2020.2979292.

[27] U. C. Hasar, A. Muratoglu, M. Bute, J. J. Barroso, and M. Ertugrul, "Effective constitutive parameters retrieval method for bianisotropic metamaterials using waveguide measurements," *IEEE Trans. Microw. Theory Techn.*, vol. 65, no. 5, pp. 1488–1497, May 2017, doi: 10.1109/TMTT.2016.2644639.

[28] E. Rephaeli and S. Fan, "Absorber and emitter for solar thermo-photovoltaic systems to achieve efficiency exceeding the Shockley-Queisser limit," *Opt. Exp.*, vol. 17, no. 17, pp. 15145–15159, Aug. 2009, doi: 10.1364/OE.17.015145.

[29] Y. Xie, X. Fan, J. D. Wilson, R. N. Simons, Y. Chen, and J. Q. Xiao, "A universal electromagnetic energy conversion adapter based on a metamaterial absorber," *Sci. Rep.*, vol. 4, no. 1, p. 6301, Sep. 2014, doi: 10.1038/srep06301.

[30] E. L. Jacobs and R. H. Lang, "Scattering, transmission, and absorption by a rough resistive sheet–E polarization," *IEEE Trans. Antennas Propag.*, vol. 50, no. 11, pp. 1567–1576, Nov. 2002, doi: 10.1109/TAP.2002.803967.

[31] E. F. Knott and C. D. Lunden, "The two-sheet capacitive Jaumann absorber," *IEEE Trans. Antennas Propag.*, vol. 43, no. 1, pp. 1339–1343, Nov. 1995, doi: 10.1109/8.475112.

[32] Z. Chen, H. Bayat, and A. Adhyapak, "Multiphysics analysis of RF pyramidal absorbers," in *Proc. Antenna Meas. Techn. Assoc. Symp. (AMTA)*, Oct. 2019, pp. 1–6, doi: 10.23919/AMTAP.2019.8906386.

[33] J. Cao, F. Xie, E. Ding, X. Zhang, P. Qian, and K. He, "Temperature characteristics of the valve-controlled shock absorber," in *Proc. IEEE 8th Int. Conf. Fluid Power Mechatronics (FPM)*, Apr. 2019, pp. 666–670, doi: 10.1109/FPM45753.2019.9035857.

[34] A. Kumar R., C. Saha, and R. Sethunadh, "Dual band energy harvester based on metasurface absorber," in *Proc. URSI Regional Conf. Radio Sci. (URSI-RCRS)*, Feb. 2020, pp. 1–4, doi: 10.23919/URSIRCRS49211.2020.9113602.

[35] M. M. Gajibo, M. K. A. Rahim, N. A. Murad, O. Ayop, and H. A. Majid, "ASingle and dual band metamaterial switchable absorber or reflector," in *Proc. IEEE Asia Pacific Microw. Conf. (APMC)*, Nov. 2017, pp. 509–512, doi: 10.1109/APMC.2017.8251493.

[36] A. Hoque, M. T. Islam, R. Azim, M. J. Singh, K. Mat, and M. Cho, "A new split pitch square shape metamaterial absorber for X band application," in *Proc. 6th Int. Conf. Space Sci. Commun. (IconSpace)*, Jul. 2019, pp. 85–90, doi: 10.1109/IconSpace.2019.8905969.

[37] S.-C. Tian, H. Xue, and L. Li, "An broadband transparent metamaterial absorber using an ITO resistive-film," in *Proc. Int. Workshop Antenna Technol. (iWAT)*, Mar. 2018, pp. 1–3, doi: 10.1109/IWAT.2018.8379144.

[38] X.-Y. Ling, Z.-Y. Xiao, X.-X. Zheng, J.-Y. Tang, and K.-K. Xu, "A broadband and polarization-insensitive metamaterial absorber," in *Proc. Prog. Electromagn. Res. Symp. (PIERS)*, Aug. 2016, pp. 3084–3087, doi: 10.1109/PIERS.2016.7735197.

[39] S. McLaren, I. Kilen, and J. V. Moloney, "Microscopic charge carrier dynamics within non-normal incidence VECSEL cavities," *Proc. SPIE*, vol. 11704, Mar. 2021, Art. no. 117040H.

[40] J. Ren, S. Gong, and W. Jiang, "Low-RCS monopolar patch antenna based on a dual-ring metamaterial absorber," *IEEE Antennas Wireless Propag. Lett.*, vol. 17, no. 1, pp. 102–105, Jan. 2018, doi: 10.1109/LAWP.2017.2776978.

[41] A. K. Singh, M. P. Abegaonkar, and S. K. Koul, "Dual- and triple-band polarization insensitive ultrathin conformal metamaterial absorbers with wide angular stability," *IEEE Trans. Electromagn. Compat.*, vol. 61, no. 3, pp. 878–886, Jun. 2019, doi: 10.1109/TEMC.2018.2839881.

[42] X. Huang, C. Lu, C. Rong, Z. Hu, and M. Liu, "Multiband ultrathin polarization-insensitive terahertz perfect absorbers with complementary metamaterial and resonator based on high-order electric and magnetic resonances," *IEEE Photon. J.*, vol. 10, no. 6, pp. 1–11, Dec. 2018, doi: 10.1109/JPHOT.2018.2878455.

[43] T. Irimatsugawa, S. Hatakeyama, M. Ohno, H. Takahashi, C. Otani, and T. Maekawa, "High energy gamma-ray spectroscopy using transition-edge sensor with a superconducting bulk tantalum absorber," *IEEE Trans. Appl. Supercond.*, vol. 25, no. 3, pp. 1–3, Jun. 2015, doi: 10.1109/TASC.2014.2380173.

[44] A. V. Uskov, J. R. Karin, J. E. Bowers, J. G. McInerney, and J. Le Bihan, "Effects of carrier cooling and carrier heating in saturation dynamics and pulse propagation through bulk semiconductor absorbers," *IEEE J. Quantum Electron.*, vol. 34, no. 11, pp. 2162–2171, Nov. 1998, doi: 10.1109/3.726609.

[45] S. Z. Islam, M. L. Othman, M. Saufi, R. Omar, A. Toudeshki, and S. Z. Islam, "Photovoltaic modules evaluation and dry-season energy yield prediction model for NEM in Malaysia," *PLoS ONE*, vol. 15, no. 11, Nov. 2020, Art. no. e0241927.
[46] S. Z. Islam, M. L. Othman, N. Mariun, H. Hizam, and N. Ayuni, "Feasibility analysis of standalone PV powered battery using SEN for smart grid," *Int. J. Power Electron. Drive Syst. (IJPEDS)*, vol. 11, no. 2, p. 667, Jun. 2020.

MD JASIM UDDIN (Member, IEEE) received the bachelor's degree from the Asian University of Bangladesh, the master's by research degree from International Islamic University Malaysia (IIUM), and the Ph.D. degree from Queensland University of Technology, Brisbane, Australia. He is a passionate Early Career Researcher. Recently, he joined Cardiff School of Technologies, Cardiff Metropolitan University, as a Lecturer. He was awarded several prestigious research grants from several countries, including Australia and Malaysia. He was awarded QUTPRA and "HDR Research" to secure his Ph.D. degree. During his doctoral study, he was also awarded an industry research scholarship from the Commonwealth Scientific Industrial Research Organization (CSIRO). Before joining QUT, he was a Faculty Lecturer, a Course Coordinator, and a Thesis/Project Committee Secretory at the Asian University of Bangladesh. He taught various electronic related courses in various universities, including Monash University, Queensland University of Technology, and International Islamic University Malaysia. He has a broad experience in supervising undergraduate and postgraduate students in respective universities. He has an extensive experience in international collaboration both industry and academia at international scale. He authored and coauthored more than 25 articles, including 17 journals, eight conferences, one book, one book chapter, and presented his research in many international conferences, workshops, and seminars as a keynote speaker. His research interests include RF, microwave, THz, and electromagnetic application. He is a regular reviewer of several reputed journals in the areas of electromagnetic fields.

MOHAMMAD HABIB ULLAH received the Ph.D. degree in electrical, electronic, and systems engineering from Universiti Kebangsaan Malaysia, Selangor, Malaysia. He is currently working as a Postdoctoral Research Fellow with the Faculty of Engineering, University of Malaya, Malaysia. He has published 64 research articles in journals, contributed as an author/coauthor. His research interest includes physical science engineering. His main area of expertises include antenna and propagation, electromagnetics, metamaterials, energy harvesting, biocomposite materials, and RF and microwave.

SYED ZAHURUL ISLAM received the master's degree in electrical engineering from Universiti Tenaga Nasional, Malaysia, in 2011, and the Ph.D. degree in electrical engineering from Universiti Putra Malaysia (UPM), in 2016. He is currently a Senior Lecturer with the Faculty of Electrical and Electronics Engineering, Universiti Tun Hussein Onn Malaysia. He is involved in collaborative research with ALPER (UPM) and BioSiliconMed Inc., Canada, for many years. Besides academic and research experience, he is experienced in program development and review curriculum for electrical and computer engineering program. His research interests include green and sustainable energy, photovoltaic cooling systems, wireless communication, sensing technology, smart grid, and smart agriculture farming. He is affiliated with IET as a member. In IEEE conferences, journals, and other scientific publications, he has served as an invited reviewer.